ELSEVIER

Automation in Construction 17 (2007) 45 – 55

AUTOMATION IN CONSTRUCTION

www.elsevier.com/locate/autcon

Cable-suspended robotic contour crafting system

Paul Bosscher [a], Robert L. Williams II [a,*], L. Sebastian Bryson [b], Daniel Castro-Lacouture [b]

[a] *Department of Mechanical Engineering, Ohio University, Athens, Ohio 45701, United States*
[b] *Department of Civil Engineering, Ohio University, Athens, Ohio 45701, United States*

Accepted 20 February 2007

Abstract

This article introduces a new concept for a contour crafting construction system. Contour crafting is a relatively new layered fabrication technology that enables automated construction of whole structures. The system proposed here consists of a mobile contour crafting platform driven by a translational cable-suspended robot. The platform includes an extrusion system for laying beads of concrete as well as computer-controlled trowels for forming the beads as they are laid. This system is fully automated and its goal is to construct concrete structures rapidly and economically. The novel attributes of this system potentially enable significant improvements over other proposed contour crafting systems, including better portability, lower cost, and the possibility to build much larger structures. This article presents the kinematics and statics of the proposed system, provides a proof of translation-only motion, and uses the reachable workspace of the robot as well as the corresponding cable tensions to approximate the maximum size structure that can be built using this manipulator.

Keywords: Contour crafting; Concrete extrusion; Cable-suspended robot; Workspace; Translation-only robot

1. Introduction

Contour crafting (CC) is a layered fabrication technology that has been proposed by Khoshnevis [1,2] for automated construction of civil structures. The aim of this technology is to improve the speed, safety, quality and cost of building construction.

Similar to other layered fabrication technologies such as rapid prototyping, stereolithography and solid free-form fabrication, CC uses a computer controlled process to fabricate structures by depositing layers of material, building the structure from the ground up, one layer at a time. However, unlike existing layered fabrication processes, CC is designed for construction of very large scale structures, on the scale of single-family homes up to housing complexes and office buildings. Fig. 1 shows a schematic (from [1]) showing a building being constructed using CC.

The CC process involves depositing strips/beads of material (typically a thick concrete/paste type material) using an extrusion process. A nozzle (shown in yellow in Fig. 1) extrudes the material in the desired locations. In the original formulation of this system the x–y–z position of the nozzle is controlled by a Cartesian gantry manipulator. This article will present an alternative manipulator for performing this task.

As the nozzle moves along the walls of the structure the construction material is extruded and troweled using a set of actuated, computer controlled trowels. The use of computer-controlled trowels allows smooth and accurate surfaces to be produced. Fig. 2 shows a close-up of the extrusion/troweling tool in a small-scale prototype CC system developed by Koshnevis (from [1]).

Because of the highly automated nature of CC, it has the potential to significantly increase the speed and decrease the cost of concrete structure construction. This technique also greatly increases design flexibility, as architects would be able to design structures with complex geometries that would be difficult to construct using current concrete construction techniques. In addition to automated deposition of concrete-like materials, the system could be modified to allow automated

* Corresponding author. Tel.: +1 740 593 1096; fax: +1 740 593 0476.
E-mail addresses: bosscher@ohio.edu (P. Bosscher), williar4@ohio.edu (R.L. Williams), bryson@ohio.edu (L.S. Bryson), castro-l@ohio.edu (D. Castro-Lacouture).

0926-5805/$ - see front matter © 2007 Elsevier B.V. All rights reserved.
doi:10.1016/j.autcon.2007.02.011

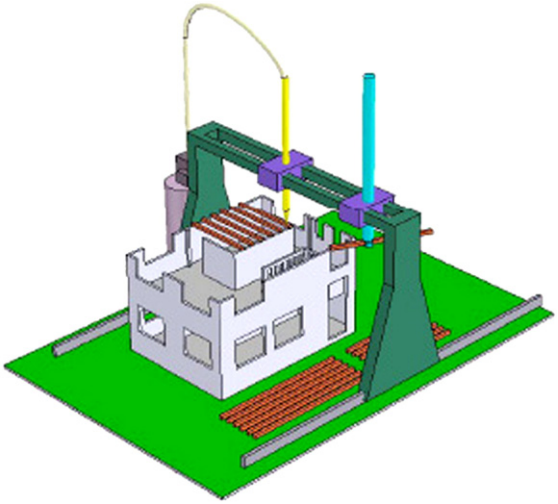

Fig. 1. Construction of a building using contour crafting and a gantry robot system (figure from [1]).

addition of reinforcement materials, plumbing and electrical wiring as the structure is being built (see [1] for more details).

The CC process relies on manipulating the extrusion/troweling nozzle through a very large workspace. Since this manipulation primarily requires only Cartesian motion, a gantry system has been proposed in [1] for performing this motion. However, in [1] it is recognized that building very large structures with a gantry robot requires an extremely large gantry robot, which may be difficult to build and implement. Indeed, such a manipulator would be relatively large and heavy, with massive actuators. It could be cumbersome to transport and deploy at a construction site. In this article an alternative manipulator is presented for performing Cartesian manipulation of a CC platform.

The outline of this article is as follows. First the use of cable robots for CC is motivated in Section 2. In Section 3 a cable robot concept, termed the Cable-Suspended Contour-Crafting Construction (C^4) Robot, is presented for performing CC tasks. The operation of the system is then described in Section 4, followed by a discussion of the robot kinematics and statics in Sections 5 and 6. Proof of translation-only motion of the manipulator is given in Section 7. The workspace of the manipulator is studied in Section 8, including an examination of the cable tensions throughout the workspace. Finally Section 9 presents some conclusions and future work.

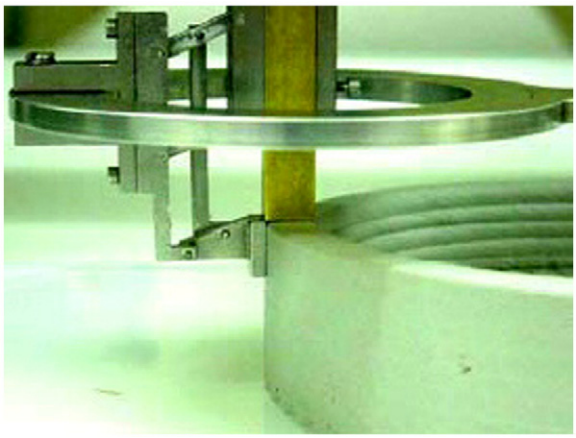

Fig. 2. Prototype of contour crafting system (figure from [1]).

2. Cable robots

Cable-driven robots (or cable-suspended robots or tendon-driven robots), referred to here as cable robots, are a type of robotic manipulator that has recently attracted interest for large workspace manipulation tasks. Cable robots are relatively simple in form, with multiple cables attached to a mobile platform or end-effector as illustrated in Fig. 3. The end-effector is manipulated by motors that can extend or retract the cables. In addition to large workspaces, cable robots are relatively inexpensive and are easy to transport, disassemble and reassemble. Cable robots have been used for a variety of applications, including material handling [3–5], haptics [7,8], and many others.

Based on the degree to which the cables determine the pose (position and orientation) of the manipulator, cable robots can be put into one of two categories: fully-constrained and underconstrained. In the fully-constrained case the pose of the end-effector can be completely determined given the current lengths of the cables. Fig. 4 shows an example of a fully-constrained cable robot, the FALCON-7 [3], a small-scale seven-cable high-speed manipulator able to achieve accelerations up to 43 g. Fully constrained cable robots have been designed for applications that require high precision, high speed/acceleration or high stiffness. Underconstrained cable robots have been proposed by the second author and NIST for contour crafting type construction [6]. However, because of the need for large workspace manipulation that has both precise motion and high stiffness, we propose the use of a fully-constrained cable robot for contour crafting.

Several other fully-constrained cable robots exist ([8–10]). However, these manipulators are only practical for small-workspace applications because the required geometry of the cables and end-effector for these manipulators are not intended for large workspaces. For example, implementing the FALCON-7 in Fig. 4 on a large scale would require a very large and cumbersome end-effector rod. In addition, fully constrained

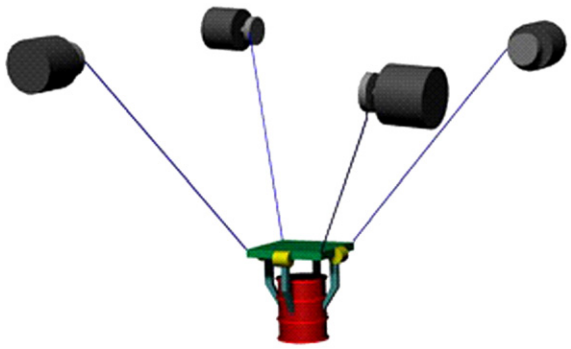

Fig. 3. Example cable robot.

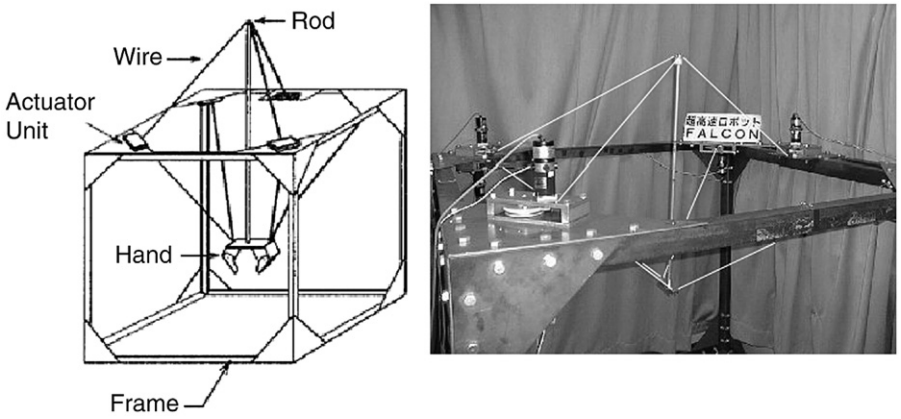

Fig. 4. Falcon-7 (figures from [3]).

cable robots often have cable interference issues, particularly with the cables colliding with nearby objects. The manipulator presented here is designed to be practical for large workspace manipulation while avoiding collisions between itself and the structures being built.

3. Contour crafting Cartesian cable robot

To perform the task of translation-only manipulation of an extrusion/construction end-effector through large workspaces for CC tasks, we are proposing the Contour Crafting Cartesian Cable Robot, abbreviated as the C^4 robot. The C^4 robot, shown in Fig. 5, consists of a rigid frame and an end-effector suspended from twelve cables, grouped into four upper cables and eight lower cables. The eight lower cables are additionally divided into four pairs of parallel cables. The arrangement of the cables is derived from a previous cable robot developed by the first two authors [12] for translation-only motion.

The cables are routed through pulleys that are mounted to a large cube-shaped frame to motors that actuate the lengths of the cables, which can be located at the base of the frame. The frame consists of truss-like members that can be easily transported and assembled at the construction site. The frame must be large enough to completely enclose the structure that is being built. The pulleys for the lower cables are mounted on horizontal crossbars, oriented at an angle of 45° with respect to the adjacent horizontal frame members, where the width of each crossbar is equal to the width of the corresponding side of the end-effector. The end-effector includes all of the extrusion and troweling tools for performing CC. The concrete is pumped from an external storage tank to the end-effector via a flexible suspended hose, as shown in Fig. 6.

The function of the upper cables is essentially to support the weight of the end-effector, while the lower cables provide the required translation-only motion. For each pair of cables, the two cables are controlled such that they have the same length (this can be easily accomplished by reeling in each pair of cables with a single motor). As a result, a parallelogram is formed by each pair of cables and the corresponding crossbar and the edge of the end-effector that the two cables connect to. By maintaining this parallelism, translation-only motion can be guaranteed, as will be shown in Section 7. This not only simplifies control of the manipulator, it also drastically reduces the complexity of the forward kinematics solution. Only three sets of the parallel cables are necessary to guarantee translation-only motion (much like the three sets of parallel links in the

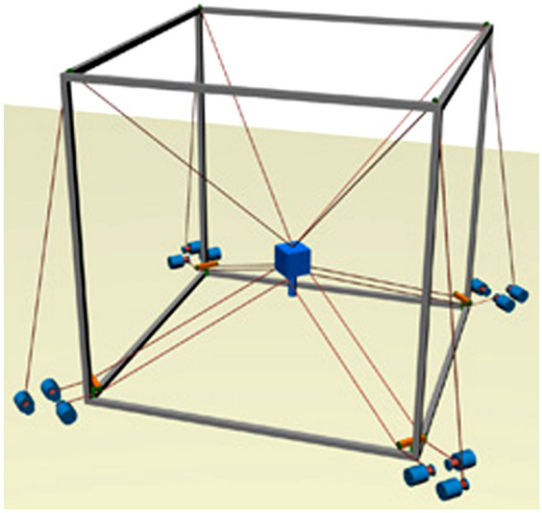

Fig. 5. The contour crafting Cartesian cable robot (C^4 robot).

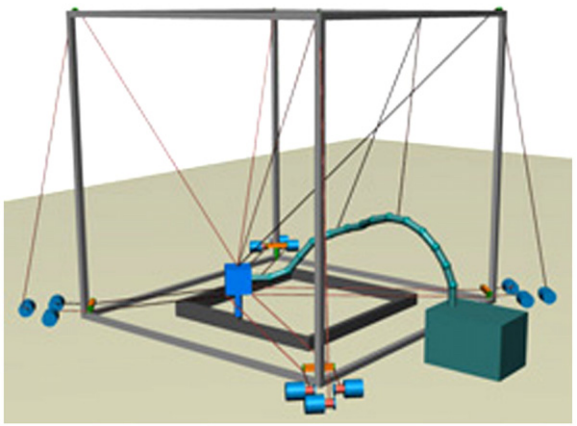

Fig. 6. C^4 robot building a structure (concrete hose and storage tank shown).

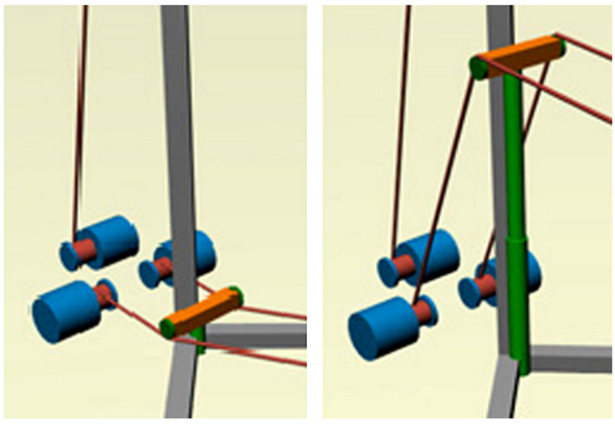

Fig. 7. Crossbar in lowered (left) and raised (right) configurations.

Delta robot [11]), however the addition of the fourth set increases the manipulator workspace.

Because the robot is fully-constrained, it can be engineered have high stiffness relative to conventional manipulators and it can be designed to exert the required construction task forces and moments. Most fully-constrained cable robots have problems with cables interfering with each other and with surrounding objects. While the arrangement of the cables prevents interference between cables, it does not prevent interference with the building being constructed. In order to solve this problem, the horizontal crossbars on the frame are actuated vertically. Each crossbar can be independently linearly actuated along the vertical edge of the frame. This enables the manipulator to continuously reconfigure itself in order to avoid collisions between the lower cables and the building. Fig. 7 shows a close-up of the actuation of one of the crossbars. The actuation of the crossbars can be accomplished a number of ways, including via hydraulic pistons, gear/chain drives or cable drives. The actuation mechanism must also be properly shrouded in order to prevent jamming due to construction debris. The configuration of the cables allows for easy translation-only motion as well as easy forward and inverse position kinematics. The eight lower cables are grouped into pairs of parallel cables. Pure translational motion is accomplished by keeping the lengths of any two paired cables the same. In addition to simplifying the kinematic equations, this simplifies control of the manipulator.

4. System operation

Using this system to construct buildings will be accomplished as follows. The system is transported to the site with all elements of the system stowed. The system will actually be quite compact when stowed because the cables can be reeled in and the frame members will likely be constructed using trusses that can be easily assembled and disassembled. Once at the construction site, the frame is assembled, the cables are strung through the pulleys and are connected to the end-effector. The most critical step in the deployment of the system is properly leveling and anchoring the frame. It may be possible to add additional adjustable supports to the bottom of the frame that would allow it to be leveled.

When the system has been anchored, the robot must be calibrated. Due to space limitations a complete calibration routine cannot be discussed here. The construction material (concrete or a similar material) must be prepared and then pumped into the end-effector (as shown in Fig. 6). Assuming a proper foundation/footing for the structure is in place, the construction of the building can now begin. With the vertically-actuated crossbars all set to their lowest height, the end-effector is controlled to move along the desired trajectory for extruding the first layer of the structure's walls. The position of the end-effector is controlled by actuation of the 12 cables, where the length of any two paired parallel cables is kept the same. As the building is constructed a layer at a time, the height of the building will increase, making collisions between the lower cables and the building more likely. Thus after several layers have been completed each of the four actuated crossbars is raised (typically the same distance for each crossbar), allowing the robot to maintain full constraint of the end-effector while preventing any collisions between cables and the building (see Fig. 8). The entire structure is constructed in a layered fashion, with the crossbars being raised periodically to avoid collisions. The end-effector will also place structural elements such as header beams for overhangs such as windows or doorframes. This can be accomplished by mounting a serial robot arm to the end-effector, similar to what is proposed in [1] (see [1] for full details on this process).

Once the structure is completed, the C^4 robot system can be moved to a different work site to build another structure. If the next structure is to be nearby, it is not necessary to disassemble the construction system. Instead, one of the horizontal bottom members of the frame can be removed and the system can be moved (e.g. by the addition of wheels to the frame) away from the first structure and to the site of the second structure. Once all construction at the site is completed, the system can again be easily disassembled and stowed in a compact travel configuration.

5. C^4 robot kinematics

In this section we present some basic kinematic equations for control of the robot. The kinematic parameters of the robot are

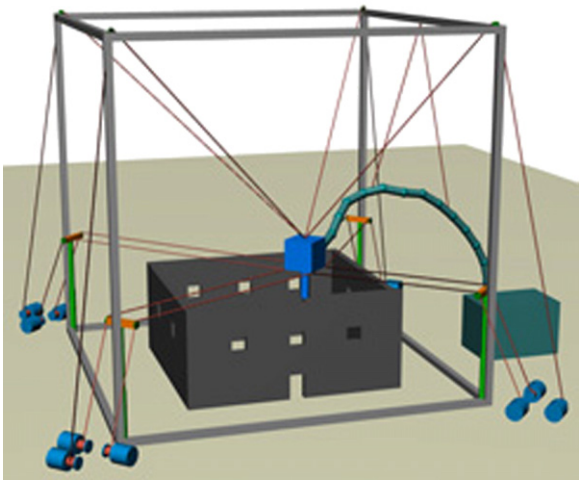

Fig. 8. C^4 robot building a structure with crossbars raised.

shown in Fig. 9. The frame is assumed to be a rectangular parallelepiped with sides of fixed length d_X, d_Y, d_Z. The base coordinate frame $\{B\}$ is attached as shown, fixed to the floor in the center of the XY plane. The end-effector is constructed of a rectangular parallelepiped with fixed side lengths p_X, p_Y, p_Z. Though this robot provides translational-only motion, the end-effector is rotated at assembly relative to the base frame. The nozzle frame $\{N\}$ is attached to the end of the extrusion nozzle; though $\{N\}$ translates relative to $\{B\}$, their orientation is constrained to be always the same. An additional frame $\{P\}$ is also parallel to $\{N\}$, but located at the geometric center of the end-effector rectangular parallelepiped (not shown in Fig. 9).

Due to the arrangement of the lower cables (the pairs of cables are parallel and the horizontal crossbar for each pair is parallel to the corresponding side of the end-effector), the orientation of the end-effector does not change, as will be proven in Section 7. The four pairs of lower cables of lengths have lengths L_1, L_2, L_3, L_4, where for pair i each of the cables have length L_i. As shown in Fig. 9, the horizontal end-effector dimensions are p_X and p_Y, which are the same as the corresponding crossbar lengths. These are actuated to different heights along the vertical sides of the frame to variable heights h_1, h_2, h_3, h_4. These heights can allow the cables to be free from interference with the house under construction. When viewed from above (as shown in Fig. 10) the crossbars and the end-effector are rotated 45° from the horizontal members of the frame. This angle was chosen to ensure workspace symmetry.

There are also four upper cables meeting in a point at the top center of the end-effector, with variable lengths L_5, L_6, L_7, L_8. These cables are routed through fixed pulleys located at the upper vertices of the frame as shown in Figs. 5, 6 and 8.

5.1. Inverse position kinematics

For parallel robots such as this 12-cable-driven robot, the inverse position kinematics is generally straight-forward. The solution simply amounts to forming the known vectors between cable connection points and calculating their Euclidian norms to determine the associated required cable lengths. Due to space limitations and the simple nature of these equations they will not be detailed here.

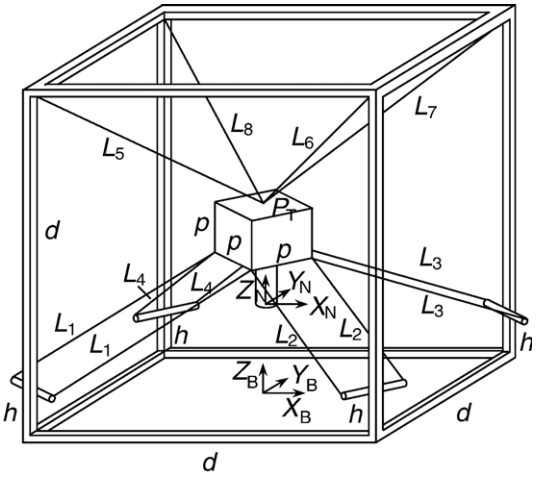

Fig. 9. Kinematic parameters of C^4 robot.

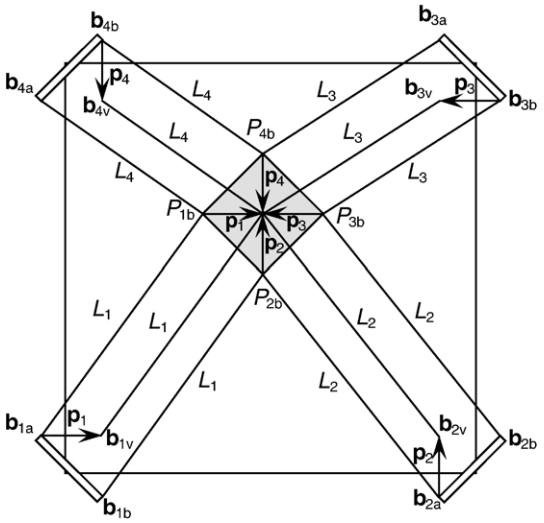

Fig. 10. Overhead view of C^4 robot with lower cables and virtual cables shown.

5.2. Virtual cable concept

The forward kinematic equations will be described next. However, we will first discuss the concept of virtual cables, which will simplify the derivation of the forward kinematic equations.

We can simplify the kinematics problems by using a single control point P located at the origin of $\{P\}$, the geometric center of the end-effector rectangular parallelepiped. For the lower four parallel cable pairs we introduce four virtual cables, in place of the eight real drive cables as follows. From cable attachment points P_{ib} on the end-effector, draw vectors $\mathbf{p}_i$ to P, $i=1,2,3,4$ (see Fig. 10). Since the platform orientation is not changing, the orientations of all $\mathbf{p}_i$ are constant. Now, from cable base points b_{ia} on the vertically-translating cable base supports, attach these same vectors $\mathbf{p}_i$ to form virtual cable pulley points b_{iv}, as shown in Fig. 10. Connect a single virtual control cable between the two tips of these two vectors $\mathbf{p}_i$, $i=1,2,3,4$. Then the length of these virtual cables is also L_i, $i=1,2,3,4$, due to the parallelism. So the real kinematics problems may be significantly simplified without loss of generality by controlling the four virtual cables L_i to translate P. Note that Fig. 10 shows the top view for clarity; all vectors shown are 3D, so their true lengths are not shown but rather the XY planar projections of their true lengths.

5.3. Forward position kinematics

The forward position kinematics problem is stated: given the twelve cable lengths L_i, calculate the desired contour-crafting nozzle position ${}^B\mathbf{P}_N = \{x_N\ y_N\ z_N\}^T$. In general, forward position kinematics for parallel (and cable-suspended) robots is very challenging, with multiple solutions. However, due to the virtual cable simplification discussed above, the current forward position kinematics solution is straight-forward and

may be solved in closed-form. The end-effector rectangular parallelepiped center P is simply the intersection of three given spheres. Using the lower virtual cables, we can choose any three of the four virtual cables $i=1,2,3,4$. Choosing the first three, the forward position kinematics solution for P is found from the intersection of the following three spheres, where each sphere is referred to as (vector center $\mathbf{c}$, scalar radius r):

$$^{B}\mathbf{P}_{P} \rightarrow (\mathbf{b}_{1v}, L_1), (\mathbf{b}_{2v}, L_2), (\mathbf{b}_{3v}, L_3) \tag{1}$$

where points $\mathbf{b}_{iv}$ are the virtual cable pulley points as shown in Fig. 10. A closed-form three spheres' intersection algorithm is presented in [13]. There are two solutions, from which the correct one may easily be selected by computer (the upper solution rather than the lower one, for the lower parallel cable pairs). There is the possibility of imaginary solutions only if the input data to the forward position problem is not consistent (i.e. sensing or modeling errors). There is an algorithmic singularity which may be avoided by proper choice of coordinate frames. Thus the forward position solution can be found by using only three virtual cables out of the 12 active cables. This is possible due to the translation-only motion of the robot. After forward position kinematics solution is found, the inverse position kinematics solution may be used to verify that the remaining cable lengths (unused in the forward position kinematics solution) are correct.

There are many alternatives for solving the forward position kinematics solution of the 12-cable robot. For example, instead of intersecting spheres from 3 of the 4 lower virtual cables we can intersect 3 of the 4 upper real cables to find point P_T (on top of the end-effector). After we have point P from forward position kinematics with the lower virtual cables (or point P_T, when using the upper cables) we can easily calculate the nozzle position.

In practice it may be possible to develop a forward position kinematics solution using all 8 cable lengths simultaneously (4 upper real and 4 lower virtual) to reduce errors in the case of real-world sensing of the cable lengths.

6. C^4 robot statics

This section presents statics modeling for the 12-cable robot. For static equilibrium the sum of external forces and moments exerted on the end-effector by the cables must equal the resultant external wrench exerted on the environment. Because of the analogous relationship between cable robots and parallel robots, the well-known Jacobian relationship can be used to express the static equations. Let $\mathbf{F}_R$ and $\mathbf{M}_R$ be the resultant force and moment, respectively, applied by the end-effector to its surroundings (due to interaction forces and moments in the contour crafting process), expressed at point P in frame $\{P\}$. Position vector $^{P}\mathbf{P}_{CG}$ gives the location of the CG relative to P. In practice $^{P}\mathbf{P}_{CG}$ can be non-zero and even changing during the process as material is pumped in and extruded out. Let $\hat{\mathbf{L}}_i$ be the unit vector along cable i, directed away from the end-effector. Let $\mathbf{p}_i$ be the position vector from the origin of $\{P\}$ to the point of connection of the ith cable to the end-effector. Then the wrench $\mathbf{W}_R$ applied by the end-effector on its surroundings is related to the vector of cable tensions $\mathbf{t}=(t_{1a}\ t_{1b}\ t_{2a}\ t_{2b}\ \cdots\ t_{4b}\ t_5\ t_6\ t_7\ t_8)^T$ according to:

$$\mathbf{A}\mathbf{t} + \begin{Bmatrix} m\mathbf{g} \\ {}^{P}\mathbf{P}_{CG} \times m\mathbf{g} \end{Bmatrix} = \mathbf{W}_R = \begin{Bmatrix} \mathbf{F}_R \\ \mathbf{M}_R \end{Bmatrix} \tag{2}$$

where the statics Jacobian $\mathbf{A}$ (expressed in $\{B\}$ coordinates) is:

$$\mathbf{A} = \begin{bmatrix} \hat{\mathbf{L}}_{1a} & \hat{\mathbf{L}}_{1b} & \hat{\mathbf{L}}_{2a} & \cdots & \hat{\mathbf{L}}_7 & \hat{\mathbf{L}}_8 \\ \mathbf{p}_{1a} \times \hat{\mathbf{L}}_{1a} & \mathbf{p}_{1b} \times \hat{\mathbf{L}}_{1b} & \mathbf{p}_{2a} \times \hat{\mathbf{L}}_{2a} & \cdots & \mathbf{p}_7 \times \hat{\mathbf{L}}_7 & \mathbf{p}_8 \times \hat{\mathbf{L}}_8 \end{bmatrix} \tag{3}$$

The gravity vector is $\mathbf{g}=\{0\ 0\ -g\}^T$ and the end-effector mass is m. The forward statics solution is Eq. (2). The inverse statics problem is more useful, calculating the required cable tensions $\mathbf{t}$ given the wrench $\mathbf{W}_R$. The statics Eq. (2) can be inverted in an attempt to support the end-effector weight while maintaining all cable tensions positive.

For cable robots with actuation redundancy, Eq. (2) is underconstrained which means that there are infinite solutions to the cable tension vector $\mathbf{t}$ to exert the required Cartesian wrench $\mathbf{W}_R$. To invert Eq. (2) we adapt the well-known particular and homogeneous solution from resolved-rate control of kinematically-redundant serial manipulators:

$$\mathbf{t} = \mathbf{A}^{+}\mathbf{W}_R + (\mathbf{I} - \mathbf{A}^{+}\mathbf{A})\mathbf{z} \tag{4}$$

where for the 12-cable robot $\mathbf{I}$ is the 12×12 identity matrix, $\mathbf{z}$ is an arbitrary 12-vector, and $\mathbf{A}^{+}=\mathbf{A}^{\mathbf{T}}(\mathbf{A}\mathbf{A}^{\mathbf{T}})^{-1}$ is the 12×6 underconstrained Moore–Penrose pseudoinverse of $\mathbf{A}$. The first term of Eq. (4) is the particular solution $\mathbf{t}_p=\mathbf{A}^{+}\mathbf{W}_R$ to achieve the desired wrench, and the second term is the homogeneous solution $\mathbf{t}_h=(\mathbf{I}-\mathbf{A}^{+}\mathbf{A})\mathbf{z}$ that projects $\mathbf{z}$ into the null space of $\mathbf{A}$. So in principle the second term of Eq. (4) may be used to increase cable tensions until all are positive, while not changing the required Cartesian wrench. To implement Eq. (4) we use MATLAB function *lsqnonneg*, which solves the least-squares problem for Eq. (2) subject to all non-negative cable tensions.

7. Translation-only motion of the robot

As described earlier, the C^4 robot produces translation-only motion of the end-effector if the lengths of any two paired cables remain equal to each other.

Proof. Consider three pairs of lower cables. For this proof we will consider cables $1a$, $1b$, $2a$, $2b$, $3a$ and $3b$ as shown in Fig. 10 (note that the subscripts a and b are not shown in the figure, but are simply used here to denote each of the two cables in a pair). Let us construct a Jacobian matrix relating the rate at which the cables are reeled in to the resulting twist (linear and angular velocity) of the end-effector:

$$\dot{\mathbf{q}} = \mathbf{J}\begin{pmatrix} \mathbf{v} \\ \boldsymbol{\omega} \end{pmatrix} \tag{5}$$

where $\dot{\mathbf{q}}=(\dot{q}_{1a}\ \dot{q}_{1b}\ \dot{q}_{2a}\ \dot{q}_{2b}\ \dot{q}_{3a}\ \dot{q}_{3b})^T$ is the vector of cable rates, $\mathbf{v}$ is the linear velocity of the end-effector (expressed in $\{B\}$), $\boldsymbol{\omega}$

is the angular velocity of the end-effector (expressed in $\{B\}$) and

$$\mathbf{J} = \begin{bmatrix} \hat{\mathbf{L}}_{1a} & \hat{\mathbf{L}}_{1b} & \hat{\mathbf{L}}_{2a} & \hat{\mathbf{L}}_{2b} & \hat{\mathbf{L}}_{3a} & \hat{\mathbf{L}}_{3b} \\ \mathbf{p}_{1a}\times\hat{\mathbf{L}}_{1a} & \mathbf{p}_{1b}\times\hat{\mathbf{L}}_{1b} & \mathbf{p}_{2a}\times\hat{\mathbf{L}}_{2a} & \mathbf{p}_{2b}\times\hat{\mathbf{L}}_{2b} & \mathbf{p}_{3a}\times\hat{\mathbf{L}}_{3a} & \mathbf{p}_{3b}\times\hat{\mathbf{L}}_{3b} \end{bmatrix}^T. \tag{6}$$

Note that due to the parallelism of the cables $\hat{\mathbf{L}}_{ia}=\hat{\mathbf{L}}_{ib}$ for $i=1, 2, 3$. If we assume the manipulator starts from a pose where cables ia and ib have the same length ($L_{ia}=L_{ib}$; $i=1, 2, 3$) and constrain the actuation of the cables such that $L_{ia}=L_{ib}$ for any motion, then we can differentiate this relation to get

$$\dot{q}_{ia} = \dot{q}_{ib}, i = 1, 2, 3 \tag{7}$$

Consider the case where we actuate the lengths of only cables $1a$ and $1b$ while holding the other lengths fixed: $\dot{\mathbf{q}}_1=(\dot{q}_1\ \dot{q}_1\ 0\ 0\ 0\ 0)^T$. Then

$$\dot{\mathbf{q}}_1 = \mathbf{J}\begin{pmatrix} \mathbf{v}_1 \\ \boldsymbol{\omega}_1 \end{pmatrix}. \tag{8}$$

We anticipate a solution for $(\mathbf{v}_1\ \boldsymbol{\omega}_1)^T$ that results only in translation, so we assume for now that $\boldsymbol{\omega}_1=\overline{0}=(0\ 0\ 0)^T$. Eq. (8) represents a set of six equations. We examine the four equations resulting from the bottom four rows of $\mathbf{J}$:

$$0 = [(\hat{\mathbf{L}}_{2a})^T(\mathbf{p}_{2a}\times\hat{\mathbf{L}}_{2a})^T]\begin{pmatrix} \mathbf{v}_1 \\ \overline{0} \end{pmatrix} \tag{9}$$

$$0 = [(\hat{\mathbf{L}}_{2b})^T(\mathbf{p}_{2b}\times\hat{\mathbf{L}}_{2b})^T]\begin{pmatrix} \mathbf{v}_1 \\ \overline{0} \end{pmatrix} \tag{10}$$

$$0 = [(\hat{\mathbf{L}}_{3a})^T(\mathbf{p}_{3a}\times\hat{\mathbf{L}}_{3a})^T]\begin{pmatrix} \mathbf{v}_1 \\ \overline{0} \end{pmatrix} \tag{11}$$

$$0 = [(\hat{\mathbf{L}}_{3b})^T(\mathbf{p}_{3b}\times\hat{\mathbf{L}}_{3b})^T]\begin{pmatrix} \mathbf{v}_1 \\ \overline{0} \end{pmatrix}. \tag{12}$$

Using the fact that $\hat{\mathbf{L}}_{ia}=\hat{\mathbf{L}}_{ib}$ for $i=1, 2, 3$, it is straightforward to see that if $(\hat{\mathbf{L}}_{2a})^T\ \mathbf{v}_1=0$ and $(\hat{\mathbf{L}}_{3a})^T\ \mathbf{v}_1=0$ (i.e. $\mathbf{v}_1$ is perpendicular to both $\hat{\mathbf{L}}_{2a}$ and $\hat{\mathbf{L}}_{3a}$) then Eqs. (9)–(12) are satisfied. If we now examine the first two equations (resulting from the first two rows of $\mathbf{J}$), and use the fact that $\hat{\mathbf{L}}_{1a}=\hat{\mathbf{L}}_{1b}$ we get two identical equations:

$$\dot{q}_1 = (\hat{\mathbf{L}}_{1a})^T\mathbf{v}_1. \tag{13}$$

Thus the $(\mathbf{v}_1\ \boldsymbol{\omega}_1)^T$ that solve Eq. (8) can be found, where $\boldsymbol{\omega}_1=\overline{0}=(0\ 0\ 0)^T$, the direction of $\mathbf{v}_1$ is found as perpendicular to both $\hat{\mathbf{L}}_{2a}$ and $\hat{\mathbf{L}}_{3a}$, and the magnitude of $\mathbf{v}_1$ is then found from Eq. (13). Because $\mathbf{J}$ is a square non-singular matrix, this solution is a unique solution of Eq. (8), and thus our assumption of $\boldsymbol{\omega}_1=\overline{0}=(0\ 0\ 0)^T$ was correct.

Similar analyses can be performed to determine the twist of the end-effector for actuation of only the second set of cables (where $\dot{\mathbf{q}}_2=(0\ 0\ \dot{q}_2\ \dot{q}_2\ 0\ 0)^T$) and actuation of only the third set of cables (where $\dot{\mathbf{q}}_3=(0\ 0\ 0\ 0\ \dot{q}_3\ \dot{q}_3)^T$). These analyses also result in motion of the end-effector where $\boldsymbol{\omega}_2=\boldsymbol{\omega}_3=\overline{0}=(0\ 0\ 0)^T$. Now due to the linearity of Eq. (5), any solution of Eq. (5) where $\dot{q}_{ia}=\dot{q}_{ib}$, $i=1,2,3$ can be found as a superposition of the three solutions to the cases where only one pair of cables is actuated at a time. Each of these cases has been shown to result in $\omega=\overline{0}$, thus we can conclude that for any arbitrary allowed actuation of the cables $\omega=\overline{0}$. We can now integrate this result and conclude that if parallelism of the cables is maintained, the matrix $\mathbf{J}$ is non-singular, and the cable actuation satisfies Eq. (7), then the manipulator will not rotate and undergoes translation-only motion. □

Note that because of the geometry of the manipulator, translation of the end-effector guarantees that the cables remain parallel, thus that assumption is valid. In addition, throughout the workspace of the manipulator (which is found in Section 8) our assumption of a non-singular $\mathbf{J}$ is valid as well.

8. C^4 robot workspace

One of the key characteristics of this robot is its workspace. Specifically, we desire for the manipulator to reach and be able to perform CC tasks at any x–y–z position encompassed by the frame of the robot. Formally, we will define the workspace of the C^4 robot as the set of all x–y–z positions that the point P can attain (in $\{B\}$) while maintaining full constraint of the end-effector and being able to exert a specified set of forces and moments on its surroundings with all non-negative cable tensions and without any of the cables exceeding their upper tension limits. This has also been termed the "wrench-feasible workspace" of a cable robot [14].

In order to investigate the workspace of this robot, an example geometry was chosen and the workspace generated numerically using MATLAB. While this geometry is not necessarily exactly what will be used in practice, it is sufficiently "generic" that the resulting trends are expected to generalize. This example geometry consists of a 1 m cube end-effector manipulated within a 50 m cube frame. Due to the end-effector dimensions, each of the horizontal crossbars is 1 m wide. The end-effector has a mass of 1000 N and the maximum allowable tension in a cable is 10 kN. The space within the robot's frame is discretized into 2 m cubes. In addition to supporting the weight of the end-effector, at each position the robot is required to exert a force of ±450 N in the x, y and z directions and a moment of ±200 N m about the x, y and z axes. For each of these loading conditions the tensions in the cables are determined. Recall that the statics equations of the manipulator are underdetermined, thus the cable tensions cannot be determined uniquely. To resolve this we use MATLAB function *lsqnonneg*, which solves the least-squares problem for Eq. (2) subject to all non-negative cable tensions. The maximum single cable tension is determined for each individual loading condition, and then the overall maximum tension (the maximum single cable tension considering all of the loading conditions) is determined for the pose.

Figs. 11–17 show the results of this simulation. Fig. 11 shows the workspace of the C^4 robot with the horizontal crossbars all set to a height of 0 m. Every position that is reachable with acceptable cable tensions ($0 \le t_i \le 10$ kN) is represented by a colored box, with the color of the box representing the overall

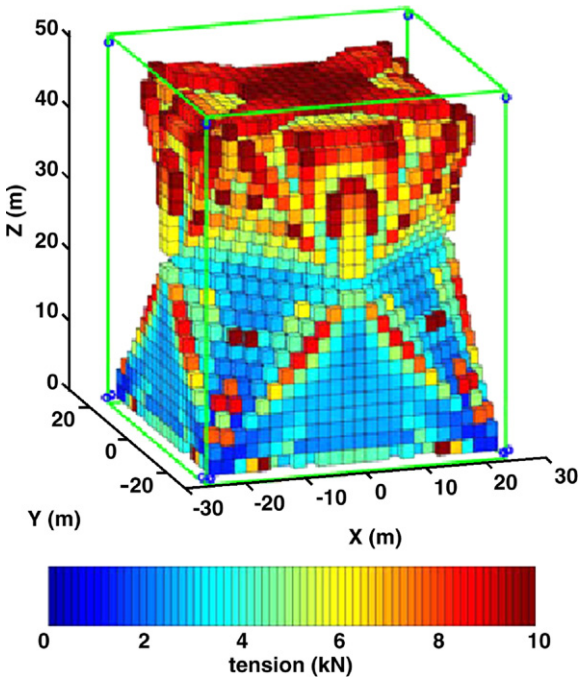

Fig. 11. Workspace of C^4 Robot with 1 m cube end-effector, colors indicate overall maximum cable tension. (For interpretation of the references to colour in this figure legend, the reader is referred to the web version of this article.)

maximum tension for the pose. The color key for Figs. 11–17 is given in Fig. 11. The robot's frame is represented by the green cube surrounding the workspace and the locations of the twelve pulleys (one for each of the twelve cables) are represented by blue circles. In Fig. 11 we can see that the workspace of the robot is quite large, filling a large majority of the volume within the frame. Due to the symmetry of the robot geometry the workspace is also symmetric.

The workspace of Fig. 11 is sliced along the $x=0$ plane and the $y=0$ plane, resulting in a quarter section of the workspace shown in Fig. 12. This section reveals that the interior of the

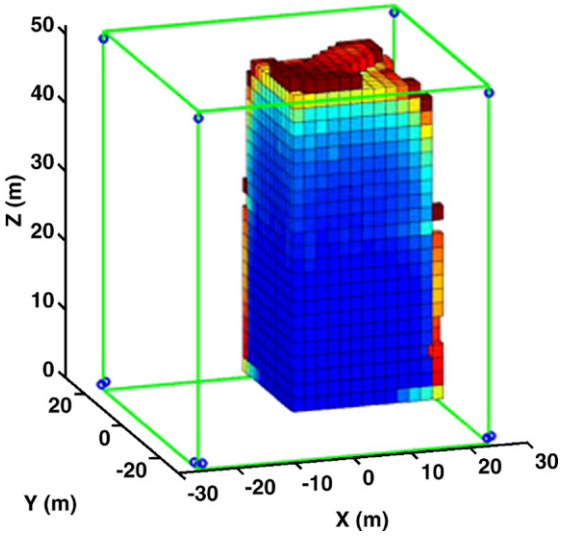

Fig. 12. Quarter section of workspace of Fig. 11.

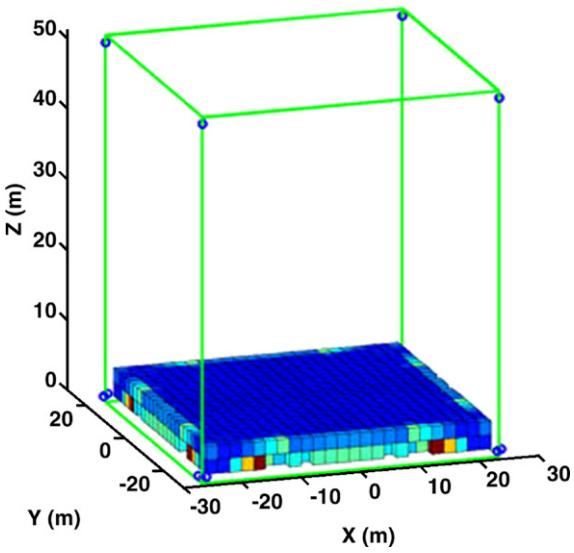

Fig. 13. Section of workspace of Fig. 11 below $Z=3$ m.

workspace has generally low tensions in the cables, which is desirable. Because the manipulator will operate low in this workspace (i.e. once the structure under construction is built up a few meters, the crossbars will be raised to avoid interference) we are particularly interested in the structure of the workspace near its bottom. Accordingly, consider Fig. 13, which is the workspace of Fig. 11 sliced along the $z=3$ m plane. Again we can see that the interior of the workspace has generally low tensions, with higher tensions only occurring near the edges of the workspace. This plot indicates that a robot of this geometry could safely construct a structure with a foundation that is contained within a roughly 44×44 m area.

As the construction of the building continues, the crossbars will need to be raised in order to avoid interference of the cables with the building under construction. The crossbars need only be raised a few meters at a time. As a representative example the

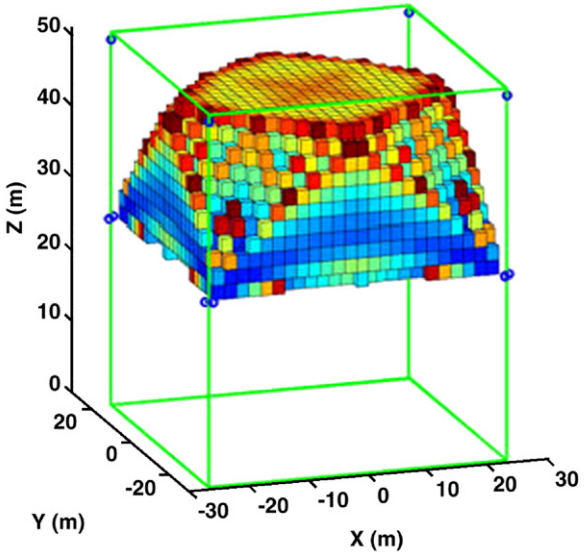

Fig. 14. Workspace of C^4 robot with crossbars moved to $Z=25$ m.

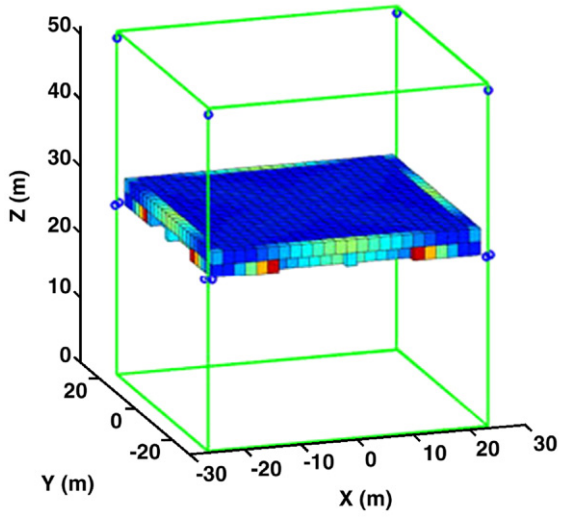

Fig. 15. Section of workspace of Fig. 14 below $Z=28$ m.

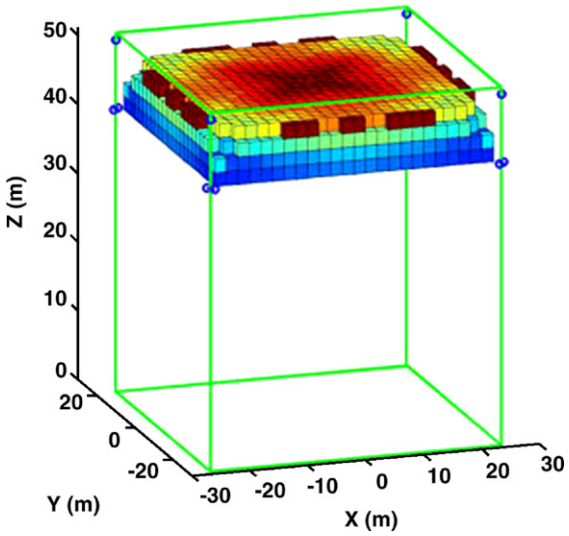

Fig. 17. Section of workspace of Fig. 16 below $Z=43$ m.

workspace of the robot is shown in Fig. 14 with the horizontal crossbars all set to a height of 25 m. Again the workspace is fairly large, filling the majority of the space from $z=25$ to 50 m in the frame. More importantly, the workspace is wide in the vicinity of $z=25$ m, where the end-effector will be operating during this stage of construction. This can be seen in Fig. 15, where the workspace of Fig. 14 is sliced along the $z=28$ m plane. Again we can see that the interior of the workspace has generally low tensions, with higher tensions only occurring near the edges of the workspace. In addition, the usable area of this portion of the workspace is still approximately 44×44 m.

Lastly, we consider the workspace of the robot with the crossbars raised to 40 m, which is near the maximum expected height for the crossbars. The resulting workspace of the robot is shown in Fig. 16. The workspace is not particularly large, however the workspace is very wide in the vicinity of $z=40$ m, where the end-effector will be operating during this stage of construction. This can be seen in Fig. 17, where the workspace of Fig. 16 is sliced along the $z=43$ m plane. The interior of this section has larger tensions than those seen in Figs. 13 and 15, but none higher than 4 kN. Given the usable area of this portion of the workspace, it appears that the maximum size building that can be constructed with this robot using our example geometry is approximately $44\times44\times40$ m, which is very effective considering the 50 m cube frame.

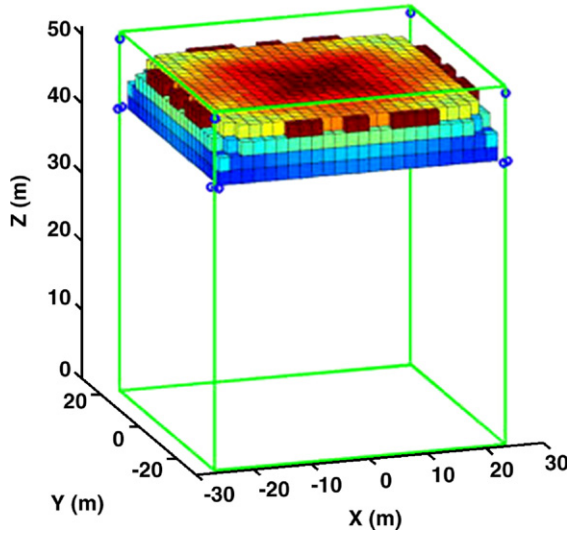

Fig. 16. Workspace of C^4 robot with crossbars moved to $Z=40$ m.

9. Cost and productivity analysis

Analysis of a typical construction operation performed with conventional methods will yield information on costs and productivity rates as a basis for comparison with the proposed CC operation. Placing and vibrating concrete is a work item shown in standard cost guides [15]. In particular, the item to be estimated consists of placing and vibrating structural concrete for a 12″ (0.305 m) thick wall, considering three situations: direct chute, pumped, and with crane and bucket. The daily output, costs and crews associated with these tasks are listed in Table 1. Costs include labor, equipment, overhead and profit average values from contractors in the United States.

Table 1 indicates an average operation cost of about US$40/$m^3$ and a productivity of 77 m^3/day. It also shows the crew composition for each task, which at its simplest situation denotes the presence of one foreman, four laborers and one cement finisher. The other situations feature a more labor-intensive environment.

The determination of costs and productivity outputs for the C^4 robot operation will be based on the hypothetical construction of a 20 m wide, 12″ (0.305 m) thick, 4 m tall foundation wall. This workspace dimension will allow the robot manipulator to fully exert CC tasks while reaching wall areas with the end-effector, as explained in the previous section ("C^4 robot workspace"). Although conventional concrete will not be the most suitable material for CC tasks due to expected problems with aggregate congestion in the nozzle, compacting difficulties, spacing limitations due to rebar and formwork

installation and other constraints due to the nature of this traditionally manual task, other materials such as self-compacted concrete will expedite concrete compaction while maintaining the quality of the structure [16]. On the other hand, extruded concrete addresses the formwork, aggregate and rebar issue by using fibers that improve the cohesion of the concrete mix [17].

In the case study of the 20 m wide, 12″ (0.305 m) thick, 4 m tall foundation wall, the C^4 robot operation will place 12″ wide (0.305 m), 2″ tall (5.08 cm) layers at a conservative speed of 1 km/h, finishing one layer in approximately 0.02 h. The CC operation for the entire foundation wall will take approximately 1.57 h, which will be rounded to 2 h due to manipulator set up, height adjustment and contingencies, about 25% of the working time. The CC productivity for the entire foundation wall operation will yield a value of approximately 12.2 m^3/h, or 97.6 m^3/day, considering an 8-h working day. For the determination of costs, a combination of concrete pump costs and manipulator operational costs will be used for this endeavor. Also, a labor foreman, responsible for overseeing the operation and monitoring the concrete supply, will be included in the estimate. The manipulator operational costs are related to the energy source used for powering the unit (e.g., grid, compressor, etc.). An estimated daily amount can be extrapolated from equivalent design elements at the bench scale level [15]: one compressor (US$120), one 25-ton crane (US$651), one concrete conveyor (US$152), one small concrete pump (US$700) and one labor foreman ($185). This yields a total of US$1808/day. Cost data for the manipulator control operations, including electronic instrumentation and tension mechanisms are still uncertain. However, a preliminary estimate of US$2,000/day will be used for comparison. Using the productivity of 97.6 m^3/day estimated earlier, the cost per m^3 is estimated to be about US $39. This estimate is greater than the current method of direct chute (US$24) and the same as the pumping method (US$39), but is lower than the labor-intensive operation with crane and bucket (US$57). In summary, Table 2 shows the cost and productivity comparison for conventional vs. CC construction, for the case illustrated.

The conventional task depicted in Table 2 corresponds to the average values of Table 1, but including the crew for the direct chute, which the least labor-intensive. The CC task presents a higher daily output when compared to the conventional task (27% greater). The CC cost is very similar to the conventional operation. Although the values used for the robot manipulator are approximated to its conversion from a bench scale operation, these values are still conservative. Furthermore, there are additional costs that could be saved in the CC operation. Accident costs, safety training, and labor burden are considerable costs that are not estimated upfront. CC is a more economical alternative, since these costs are not as significant as in the conventional concrete operation task.

Table 1
Cost and productivity data for placing and vibrating 12″ wall concrete (adapted from [15])

Task	Crew	Daily output (m^3/day)	Cost (US$/$m^3$)
Direct chute	1 foreman, 4 laborers, 1 cement finisher	77	24
Pumped	1 foreman, 5 laborers, 1 cement finisher, 1 equipment operator	85	39
With crane and bucket	1 foreman, 5 laborers, 1 cement finisher, 1 equipment operator, 1 equipment oiler	69	57
Average		77	40

Table 2
Cost and productivity comparison

Task	Crew	Daily output (m^3/day)	Cost (US$/$m^3$)
Conventional	1 foreman, 4 laborers, 1 cement finisher	77	40
CC	1 foreman	98	39

10. Conclusions and future work

This article has presented a new cable robot, the C^4 robot, designed for use in a contour crafting system. It combines several novel features, including a geometry that permits translation-only motion and highly simplified kinematic equations, and the use of actuated cable mounts that allow on-line reconfiguration of the cable robot to eliminate cable interference while maintaining full constraint of the end-effector. This system can be engineered to provide the ability to contour-craft large structures with the potential for being less expensive and more portable than existing robot concepts for contour crafting.

The forward and inverse position kinematics solutions were discussed, which incorporated the concept of virtual cables in order to simplify the forward position kinematics. The static equations were presented, including a discussion of how the redundancy of the manipulator can be used to maintain non-negative tensions in all cables. The manipulator's workspace was investigated for an example geometry, including calculation of the maximum cable tension for a variety of loading conditions. The workspace was determined to be potentially very large, with low maximum cable tensions for nearly all positions. Based on this workspace analysis, it was concluded that the frame of the robot only needs to be slightly larger than the building being constructed. Lastly, an initial cost and productivity analysis was presented, which must be updated as this concept and the construction industry progresses.

Future plans for manipulator development include constructing a small-scale prototype, detailed mechanical design of the system components, and development of calibration routines and automated controller. Additional work is also planned on improved construction materials and extrusion/troweling tooling.

References

[1] B. Khoshnevis, Automated construction by contour crafting — related robotics and information technologies, Journal of Automation in Construction — Special Issue: The Best of ISARC 2002 13 (1) (January 2004) 5–19.

[2] B. Khoshnevis, R. Russel, H. Kwon, S. Bukkapatnam, Crafting large prototypes, IEEE Robotics & Automation Magazine (September 2001) 33–42.
[3] S. Kawamura, W. Choe, S. Tanaka, S. Pandian, Development of an ultrahigh speed robot FALCON using wire drive system, Proceedings of the 1993 IEEE International Conference on Robotics and Automation, vol. 1, May 1995, pp. 215–220, Nagoya, Japan.
[4] J. Albus, R. Bostelman, N. Dagalakis, The NIST RoboCrane, Journal of National Institute of Standards and Technology 97 (3) (May–June 1992).
[5] J.J. Gorman, K.W. Jablokow, D.J. Cannon, The cable array robot: theory and experiment, Proceedings of the 2001 IEEE International Conference on Robotics and Automation, 2001, pp. 2804–2810.
[6] R.L. Williams II, J. Albus, R. Bostelman, Self-contained automated construction deposition system, Automation in Construction 13 (2004) 393–407.
[7] C. Bonivento, A. Eusebi, C. Melchiorri, M. Montanari, G. Vassura, WireMan: a portable wire manipulator for touch-rendering of bas-relief virtual surfaces, Proceedings of the 1997 International Conference on Advanced Robotics (ICAR 97), 1997, pp. 13–18.
[8] R.L. Williams II, Cable-suspended haptic interface, International Journal of Virtual Reality 3 (3) (1998) 13–21.
[9] K. Maeda, S. Tadokoro, T. Takamori, M. Hiller, R. Verhoeven, On design of a redundant wire-driven parallel robot WARP manipulator, Proceedings of the 1999 IEEE International Conference on Robotics and Automation, (Detroit, Michigan), May 1999, pp. 895–900.
[10] S. Tadokoro, Y. Murao, M. Hiller, R. Murata, H. Kohkawa, T. Matsushima, A motion base with 6-DOF by parallel cable drive architecture, IEEE/ASME Transactions on Mechatronics 7 (June 2002) 115–123.
[11] R. Clavel, Delta: a fast robot with parallel geometry, Proceedings of the 18th International Symposium on Industrial Robot, 1988.
[12] P. Bosscher, R.L. Williams II, M. Tummino, A concept for rapidly-deployable cable robot search and rescue systems, Proceedings of the 2005 ASME DETC/CIE Conferences, (Long Beach, California), DETC2005-84324, September 2005.
[13] R.L. Williams II, J.S. Albus, R.V. Bostelman, 3D cable-based Cartesian metrology system, Journal of Robotic Systems 21 (5) (2004) 237–257.
[14] P. Bosscher, 2004. “Disturbance robustness measures and wrench-feasible workspace generation techniques for cable-driven robots”. PhD thesis, Georgia Institute of Technology, Atlanta, GA, November.
[15] R.S. Means, Open shop building construction cost data, 22nd Annual Edition, 03300, Cast-in-Place Concrete, RS Means CMD Group, 2006.
[16] H. Okamura, M. Ouchi, Self-compacting concrete, Journal of Advanced Concrete Technology 1 (15) (2003) 5–15.
[17] V. Li, Large volume, high-performance applications of fibers in civil engineering, Journal of Applied Polymer Science 83 (3) (2001) 660–686.